PROCEEDINGS B

royalsocietypublishing.org/journal/rspb

Research

Cite this article: Valadez-Ingersoll M, Aguirre Carrión PJ, Bodnar CA, Desai NA, Gilmore TD, Davies SW. 2024 Starvation differentially affects gene expression, immunity and pathogen susceptibility across symbiotic states in a model cnidarian. *Proc. R. Soc. B* **291**: 20231685.
https://doi.org/10.1098/rspb.2023.1685

Received: 29 July 2023
Accepted: 29 January 2024

Subject Category:
Genetics and genomics

Subject Areas:
immunology, molecular biology, genomics

Keywords:
starvation, symbiosis, immunity, stress, NF-κB, Cnidaria

Authors for correspondence:
Thomas D. Gilmore
e-mail: gilmore@bu.edu
Sarah W. Davies
e-mail: daviessw@bu.edu

†Present address: Generate Biosciences, 101 South Street, Somerville, MA 02143, USA.

Electronic supplementary material is available online at https://doi.org/10.6084/m9.figshare.c.7075463.

THE ROYAL SOCIETY PUBLISHING

Starvation differentially affects gene expression, immunity and pathogen susceptibility across symbiotic states in a model cnidarian

Maria Valadez-Ingersoll, Pablo J. Aguirre Carrión†, Caoimhe A. Bodnar, Niharika A. Desai, Thomas D. Gilmore and Sarah W. Davies

Department of Biology, Boston University, 5 Cummington Mall, Boston, MA 02215, USA

MV-I, 0000-0002-2884-5350; NAD, 0009-0007-4030-4040; TDG, 0000-0002-1910-768X; SWD, 0000-0002-1620-2278

Mutualistic symbioses between cnidarians and photosynthetic algae are modulated by complex interactions between host immunity and environmental conditions. Here, we investigate how symbiosis interacts with food limitation to influence gene expression and stress response programming in the sea anemone *Exaiptasia pallida* (Aiptasia). Transcriptomic responses to starvation were similar between symbiotic and aposymbiotic Aiptasia; however, aposymbiotic anemone responses were stronger. Starved Aiptasia of both symbiotic states exhibited increased protein levels of immune-related transcription factor NF-κB, its associated gene pathways, and putative target genes. However, this starvation-induced increase in NF-κB correlated with increased immunity only in symbiotic anemones. Furthermore, starvation had opposite effects on Aiptasia susceptibility to pathogen and oxidative stress challenges, suggesting distinct energetic priorities under food scarce conditions. Finally, when we compared starvation responses in Aiptasia to those of a facultative coral and non-symbiotic anemone, 'defence' responses were similarly regulated in Aiptasia and the facultative coral, but not in the non-symbiotic anemone. This pattern suggests that capacity for symbiosis influences immune responses in cnidarians. In summary, expression of certain immune pathways—including NF-κB—does not necessarily predict susceptibility to pathogens, highlighting the complexities of cnidarian immunity and the influence of symbiosis under varying energetic demands.

1. Introduction

Reef-building corals are assemblages of cnidarian host cells, intracellular photosynthetic algae (Family Symbiodiniaceae) and a complex microbiome [1]. These symbioses enable corals to flourish in nutrient-poor waters [2]. In a healthy cnidarian–algal symbiosis, the symbiont provides fixed carbon photosynthates to the host while the host provides CO_2 and other essential nutrients (e.g. nitrogen and phosphorus) to the symbiont [3,4]. Corals and the complex ecosystems they engineer are globally threatened by anthropogenic climate change and associated environmental perturbations including rising ocean temperatures, increased exposure to disease and changes in nutrient availability [5]. Understanding the mechanisms underlying this symbiosis is critical for predicting how cnidarians will be affected by accelerating anthropogenic changes.

Previous work has shown that the negative impacts of climate change on corals can be mitigated by nutrient acquisition from the environment through heterotrophy [6–8]. However, the reliance of the host on either form of nutrient acquisition—prey capture (heterotrophy) or translocation from the algal symbiont – is variable across taxa and environments [9]. On one extreme, cnidarians living in tropical, low-nutrient environments form obligate associations with their symbiotic algae. If this symbiosis is lost (termed 'bleaching'), hosts will eventually

starve if they cannot buffer these energetic losses with heterotrophy [5]. In bleached corals, carbon incorporation from increased rates of heterotrophy is an important mechanism for recovery [10]. Facultatively symbiotic cnidarians also exist and tend to live in higher nutrient environments, acquiring nutrients from a combination of their algae and heterotrophy. This nutrient flexibility facilitates a range of states from symbiotic to aposymbiotic (extremely low symbiont levels) depending on environmental conditions [11]. Finally, some cnidarians are non-symbiotic and never form symbiotic relationships with photosynthetic algae and rely solely on heterotrophy [11]. This continuum of symbiotic strategies probably influences how cnidarians respond to environmental challenges.

Energetic priorities probably differ across symbiotic states and may further shift under variable nutrient conditions. Previous research has demonstrated that the non-symbiotic sea anemone *Nematostella vectensis* is more susceptible to bacterial infection under starvation, which was associated with reduced expression of known innate immune pathways [12]. In obligate and facultative symbioses, maintaining the algal symbiotic relationship, even under ambient conditions, requires tradeoffs for hosts. Much research on these tradeoffs has been done in facultatively symbiotic cnidarian models, such as the sea anemone *Exaiptasia pallida* (Aiptasia) [13,14]. First, hosts must regulate symbiont cell density to control overcrowding, which is especially important when nutrient availability changes [15]. Previous work has shown that when symbiotic Aiptasia are starved, symbiont densities decrease by up to 50%, likely due to inter-algal competition for decreased host-derived nutrients [16]. Second, symbiotic hosts must balance allowing foreign algal cells to live intracellularly while also maintaining defence against harmful pathogens [17]. In general, research in symbiotic cnidarians has demonstrated that the establishment and maintenance of symbiosis requires downregulation of certain innate immune system pathways, including the transcription factor NF-κB pathway [18,19]. Thus, in symbiotic cnidarians, the nutritional benefits conferred by symbiosis are at a potential cost to the host's defence against pathogens.

Field research has shown that symbiont loss during coral bleaching can confer heightened, though transient, protection against harmful pathogens [20]. However, stress responses are complex, and symbiotic cnidarians have also been shown to have higher antioxidant enzymes (i.e. catalase and superoxide dismutase) than aposymbiotic cnidarians, suggesting greater protection against oxidative stress in symbiotic animals [21–23]. These results suggest that NF-κB and oxidative stress response pathways are regulated differently in cnidarians. Taken together, two central themes of cnidarian symbiosis emerge: (1) symbiosis modulates host immunity, and (2) heterotrophy modulates symbiosis. However, the influence of symbiosis and nutrition on immunity, and on the individual regulatory pathways of the cnidarian immune system, remains largely unexplored, but may provide insight for understanding cnidarian stress responses.

Here, we have characterized the effects of starvation on gene expression in the facultatively symbiotic sea anemone Aiptasia when it is associated with algal symbionts (symbiotic/sym) or not (aposymbiotic/apo). We used whole-organism gene expression profiling to investigate how starvation-induced modulation of immune and oxidative stress pathways impacts cnidarian susceptibility to pathogen and oxidative stress challenges. Finally, we compared starvation-induced gene expression patterns in Aiptasia to gene expression patterns under starvation in a facultatively symbiotic stony coral (*Oculina arbuscula*) and a non-symbiotic sea anemone (*N. vectensis*). Our results suggest that, in facultatively symbiotic cnidarians, there are distinct molecular regulatory mechanisms for oxidative stress, the pathogen-responsive innate immune response, and the symbiont-responsive innate immune response. Furthermore, under starvation, energetic priorities within the immune system differ between symbiotic states and by the ability of a cnidarian species to form symbiosis with Symbiodiniaceae.

2. Material and methods

(a) Aiptasia husbandry and experimental design

Symbiotic (partnered with *Symbiodinium linucheae*) and aposymbiotic adult *Exaiptasia pallida* (Aiptasia) anemones of clonal strain CC7 [24] were maintained in 35 ppt artificial seawater (ASW, Instant Ocean) in polycarbonate tanks at 25°C under a 12 h : 12 h light : dark cycle (white fluorescent light, 25 µmol photons m^{-2} s^{-1}). Aposymbiotic Aiptasia were generated via menthol bleaching at least three months prior to experimentation as described previously [25]. Aposymbiotic Aiptasia were maintained in darkness and aposymbiotic status was confirmed by lack of symbiont autofluorescence under fluorescence microscopy (Leica M165 FC). Anemones were fed three times per week with freshly hatched *Artemia* nauplii, and water changes were performed twice weekly.

To generate clonal pairs, single anemones were placed into individual wells of a 6-well plate in 10 ml ASW, relaxed on ice for 10 min, then bisected along the oral-aboral axis. After at least two weeks, bisected anemones were determined to be healed by visual confirmation of complete regeneration of the oral/tentacle disc. During recovery, anemones were maintained at 25°C with symbiotic pairs under a 12 h : 12 h light : dark cycle and aposymbiotic pairs under darkness. All clonal pairs were fed freshly hatched *Artemia* nauplii, and water changes were performed thrice weekly during regeneration.

Following regeneration, each anemone was placed into an independent well with 10 ml of 0.2 µM-filter sterilized ASW (FSW). Three days prior to use, aposymbiotic clonal pairs were moved to a 12 h : 12 h light : dark cycle for light acclimation. During the course of the two-week treatment period, anemones were maintained under a 12 h : 12 h light : dark cycle with 25 µmol photons m^{-2} s^{-1}. For starvation experiments, one individual of each clonal pair was given 30 µl of *Artemia* nauplii three times per week ('fed' control), while the other was unfed (starved). To mimic feeding in starved anemones, 30 µl of FSW was pipetted onto all individuals. Water changes were performed twice weekly. After two weeks, anemones were preserved or processed for downstream analyses. Clonal pairs were not used for susceptibility trials, but the feeding/starvation regimen with non-bisected aposymbiotic and symbiotic CC7 Aiptasia used was identical to methods described above. The experimental design is shown in figure 1*a*.

(b) RNA extraction and TagSeq processing

After two weeks of treatment, five fed/starved clonal pairs of symbiotic and aposymbiotic Aiptasia ($n = 20$) were flash frozen and preserved in 100% ethanol. Total RNA was extracted from each anemone by grinding whole anemones with pestles during tissue lysis and centrifuging at 13 000 rpm for 15 min at 4°C. Supernatant was processed by the RNAqueous Total RNA Isolation Kit (Invitrogen) per manufacturer's instructions. RNA quantity and integrity were assessed using a NanoDrop ND-1000 Spectrophotometer. Samples were normalized to 11.4 ng $µl^{-1}$ and submitted to the University of Texas at Austin

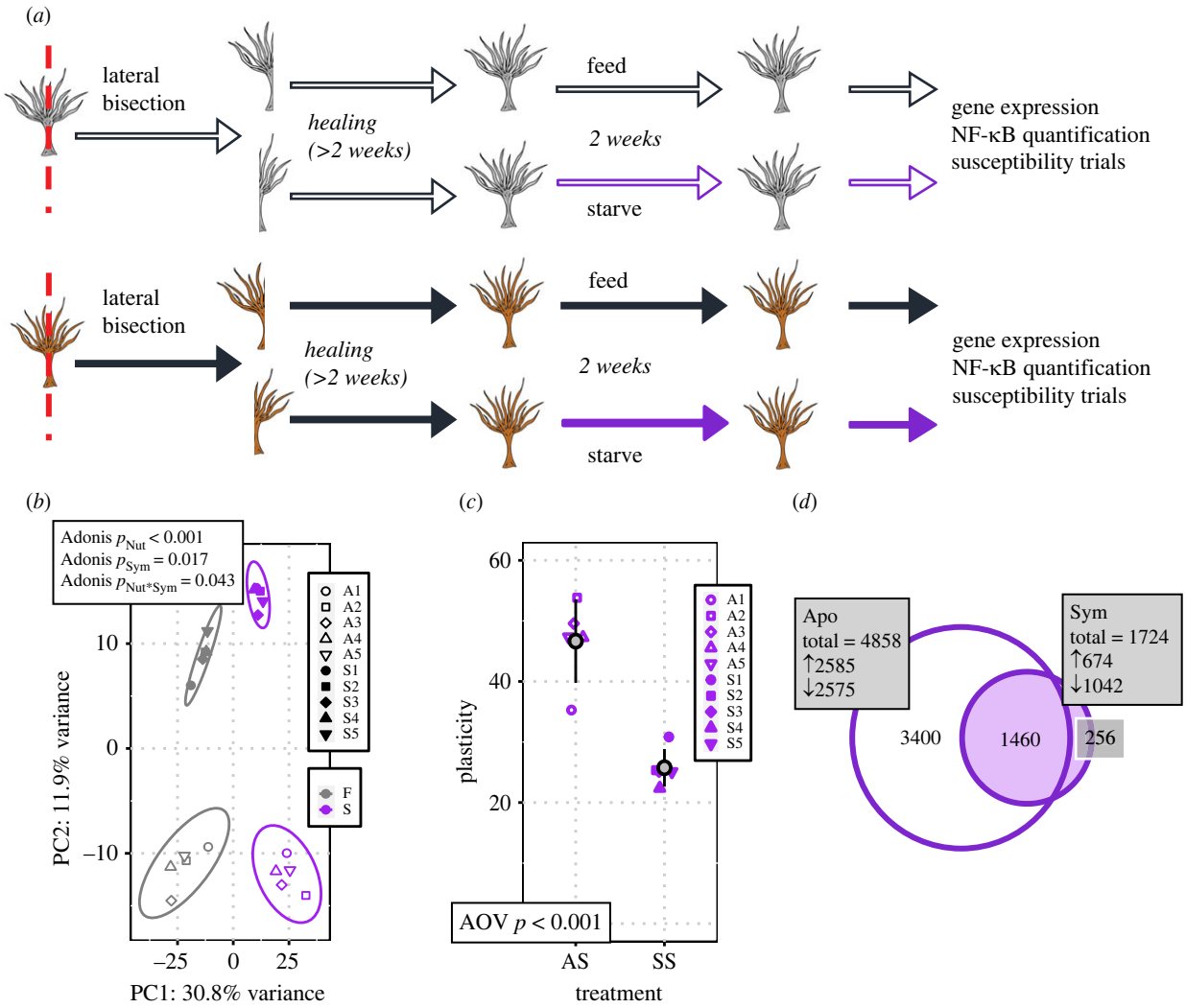

Figure 1. Starvation elicits shifts in whole-transcriptome gene expression and stronger transcriptomic responses in aposymbiotic compared to symbiotic Aiptasia. (*a*) Experimental design. Aposymbiotic (grey) and symbiotic (brown) anemones were bisected creating clonal pairs. After healing, one individual of each pair was fed regularly and the other was starved for two weeks. Individuals were then preserved for subsequent analysis. Susceptibility trial anemones were not cloned, but identical feeding/starvation conditions were employed. (*b*) Principal component analysis (PCA) of $\log_2$ transformed counts for aposymbiotic (A, open shapes) and symbiotic (S, closed shapes) Aiptasia after two weeks of feeding (F, grey) or starvation (S, purple). Fed and starved clonal pairs are indicated with unique shapes. PERMANOVA results for the effect of nutrition (p_{Nut}), symbiosis (p_{Sym}) and the interaction between nutrition and symbiotic state ($p_{Nut*Sym}$) are included. (*c*) Gene expression plasticity for aposymbiotic Aiptasia (purple open shapes) when starved (AS) and symbiotic Aiptasia (purple closed shapes) when starved (SS) was calculated using the PC distance between each fed and starved clonal pair. Grey circles show the mean and black bars indicate standard deviation. (*d*) Venn diagram of differentially expressed genes (DEGs) (FDR adjusted-*p*-value of less than 0.05) for symbiotic (Sym) and aposymbiotic (Apo) Aiptasia after starvation relative to fed control anemones.

Genomic Sequencing and Analysis Facility for TagSeq library preparation and sequencing on a NovaSeq6000 SR100.

Raw fastq reads were processed following an established pipeline (https://github.com/z0on/tag-based_RNAseq). Briefly, fastx_toolkit trimmed adapters and poly(A)$^+$ tails, PCR duplicates were removed, and short (less than 20 bp) and low-quality reads (quality score of ≤20) were discarded [26]. Cleaned reads were mapped to concatenated Aiptasia [27] and *Symbiodinium linucheae* [28] transcriptomes using Bowtie2 [23]. A raw counts file containing all genes mapping exclusively to Aiptasia was used in downstream analyses (electronic supplementary material, dataset S1). Symbiont-specific genes mapping to the *S. linucheae* reference were not analysed due to low counts.

(c) Analysis of gene expression under starvation in Aiptasia

All analyses were performed in R v.4.3.0 [29]. DESeq2 (v.1.36.0) [30] identified differentially expressed genes (DEGs) between fed and starved treatments in both symbiotic and aposymbiotic anemones by modelling all samples by treatment (ApoFed, ApoStarved, SymFed, SymStarved). ArrayQualityMetrics (v.3.52.0) [31] tested for outliers. No outliers were detected. Individual contrasts between fed and starved anemones within each symbiotic state identified DEGs (FDR-adjusted-*p* value of less than 0.05). Data were rlog-normalized and overall expression was compared through Principal Component Analysis (PCA) implemented in vegan (v.2.6-2) [32]. Gene expression similarity was tested using PERMANOVA implemented with the pairwiseAdonis package v.0.4 [33]. Gene expression plasticity of symbiotic and aposymbiotic Aiptasia under starvation was estimated as a function of the distance of each point in the treatment group (starved) relative to the location of its clonal counterpart in the control group (fed) in PC space using the first two principal components [34,35]. Gene expression plasticity for symbiotic and aposymbiotic Aiptasia was then compared using an analysis of variance. VennDiagram (v.1.7.3) [36] compared total DEGs under starvation (FDR-*p*-values of less than 0.05) in symbiotic and aposymbiotic anemones to identify DEGs shared between symbiotic states under starvation, as well as DEGs unique to the starvation responses of each symbiotic state. Expression levels of shared DEGs were correlated using a linear model of log-fold

change between starved versus fed anemones across symbiotic and aposymbiotic states.

Functional gene ontology (GO) enrichment analyses of shared DEGs and of DEGs unique to each symbiotic state under starvation were performed using Fisher Exact Tests (DEG presence/absence) [37] to identify enrichment differences across these sets of genes in the 'Biological Process' (BP) GO division [37]. Enrichment of gene pathways under starvation in symbiotic and aposymbiotic Aiptasia was independently investigated by GO enrichment analysis using the Mann–Whitney U tests (GO-MWU) [37] on all genes. Significantly enriched GO terms (FDR-*p*-value of less than 0.1) for both types of GO analyses (Fisher's exact and Mann–Whitney U-tests) were plotted in dendrograms. Significantly over and under-represented BP GO terms under starvation that were involved in the NF-κB pathway (electronic supplementary material, table S1) and superoxide or reactive oxidative stress (ROS) response pathways (electronic supplementary material, table S2) were identified. Complete lists of enriched GO terms are provided in electronic supplementary material, datasets S2 and S3. Significant DEGs (FDR-*p*-value of less than 0.05) belonging to NF-κB and ROS GO terms of interest were visualized for symbiotic and aposymbiotic samples using pheatmap v.1.0.12 [38]. Finally, we compared our gene expression dataset to a published dataset of heat-responsive Aiptasia genes (upregulated after 3 h of heat shock at 34°C) with three or more NF-κB binding sites in their promoter regions (i.e. 500 bp upstream of the transcription start site) [39] to identify possible NF-κB target genes that were significantly upregulated (FDR-*p*-value of less than 0.05) following starvation in symbiotic and aposymbiotic Aiptasia. Expression patterns were visualized using pheatmap v.1.0.12 [38].

(d) Western blotting of NF-κB

Individual anemones ($n = 12$) were homogenized in 60 µl of 2X SDS-sample buffer (0.125 M Tris-HCl [pH 6.8], 4.6% w/v SDS, 20% w/v glycerol, 10% v/v β-mercaptoethanol, 0.2% w/v bromophenol blue) using a pestle followed by heating at 95°C for 10 min. Samples were centrifuged for 10 min at 13 000 rpm and the supernatant was collected. Protein isolation and Western blotting were performed as previously described [12,18]. Extracts were electrophoresed on a 7.5% SDS-polyacrylamide gel, and proteins were transferred to a nitrocellulose membrane. The membrane was blocked for 1 h in TBST (10 mM Tris-HCl [pH 7.4], 150 mM NaCl, 0.05% v/v Tween 20 containing 5% non-fat powdered milk). The membrane was then incubated overnight at 4°C with primary rabbit-anti-Ap-NF-κB antiserum [18] (diluted 1 : 5000). The membrane was washed five times with TBST and incubated for 1 h with secondary goat-anti-rabbit-HRP conjugated antiserum (1 : 4000, Cell Signaling Technology). After further washing, immunoreactive proteins were detected with SuperSignal West Dura Extended Duration Substrate (Fisher Scientific) and imaged on a Sapphire Biomolecular Imager. Bands corresponding to Ap-NF-κB were normalized to total protein loaded in each lane using Ponceau S stain and ImageJ. For each clonal pair, total NF-κB protein in the starved individual was compared to that of its fed counterpart.

(e) Effect of starvation on pathogen- and H_2O_2-induced mortality in symbiotic and aposymbiotic Aiptasia

Pathogen susceptibility trials were performed as described previously [12] with the general pathogen *Pseudomonas aeruginosa* strain Pa14 and the opportunistic coral pathogen *Serratia marcescens* (Smarc). Pa14 and Smarc susceptibility trials were each performed in duplicate under the following conditions: symbiotic fed ($n = 24$), symbiotic starved ($n = 24$), aposymbiotic fed ($n = 24$), aposymbiotic starved ($n = 24$), comprising a total of $n = 48$ per condition and $n = 192$ total anemones per pathogen challenge. Anemones were fed or starved for two weeks, transferred to individual wells of a 24-well plate containing 1 ml FSW, and acclimated at 27°C for 24 h prior to infection. Single Pa14 and Smarc colonies were cultured overnight at 37°C in Luria Broth. Bacteria were washed three times with FSW, then diluted in FSW to an OD_{600} of approximately 0.1. FSW in 24-well plates was then replaced with 1 ml of Pa14 (approx. 3.94×10^8 CFU ml^{-1}) or 1 ml of Smarc (approx. 3.63×10^8 CFU ml^{-1}). Infected anemones were maintained at 27°C under a 12 h : 12 h light : dark cycle and monitored for viability daily for four weeks. Mortality was assessed by prevalent tissue lysis and lack of response to stimulus (touch with sterile pipette tip and water squirt). Symbiotic and aposymbiotic Aiptasia ($n = 20$) were additionally incubated in FSW at 27°C for the four-week monitoring period as experimental controls. Infected and control anemones were not fed, and water changes were not performed for the duration of the four-week exposure.

Susceptibility of fed versus starved Aiptasia to reactive oxygen species (ROS) was tested as previously described [40]. ROS susceptibility trials were performed in duplicate (symbiotic fed ($n = 24$), symbiotic starved ($n = 24$), aposymbiotic fed ($n = 24$), aposymbiotic starved ($n = 24$), comprising a total of $n = 48$ per condition and $n = 192$ total anemones). Anemones were fed or starved for two weeks, then transferred to individual wells of a 24-well plate containing 1 ml of 0.008% (2.6 mM) H_2O_2 in FSW. Daily water changes with fresh 0.008% H_2O_2 in FSW were performed, and mortality was monitored daily for four weeks. Anemones were maintained at room temperature under a 12 h : 12 h light:dark cycle and were not fed for the duration of the four-week exposure.

(f) Survival analyses

Results from duplicate pathogen and ROS susceptibility trials were analysed together using survival v.3.5-5 and survminer v.0.4.9 packages [41–43]. For each stressor, Cox proportional hazards models modelled the fixed effect of treatment (symbiotic fed (SymFed), symbiotic starved (SymStarved), aposymbiotic fed (ApoFed), and aposymbiotic starved (ApoStarved)) with a random effect of trial on the survival probability. Following this model, we conducted four pairwise comparisons: SymFed:SymStarved, ApoFed:ApoStarved, SymFed:ApoFed, and SymStarved:ApoStarved. Because multiple pairwise comparisons were completed, we employed a Bonferroni *p*-value adjustment by multiplying *p*-values by four to account for multiple comparisons.

(g) Meta-analysis of the starvation response across Cnidaria

A meta-analysis of gene expression responses to starvation across select cnidarians was performed by comparing our gene expression data to previously published datasets generated from fed/starved *N. vectensis* (non-symbiotic sea anemone) [12,41] and symbiotic *O. arbuscula* (facultatively symbiotic stony coral) [7]. We first confirmed nutrient limitation under experimental starvation conditions across experiments and then contrasted stress responses differences across taxa. All over- or under-represented BP GO terms under starvation (FDR-*p*-value of less than 0.1 from GO MWU) in two or more of the three study species were identified. This approach revealed 101 GO terms from which 37 metabolism-related terms and 6 defence-related terms were identified, and these GO term delta rank values were compared across taxa and visualized in ggplot2 (v.3.4.0) [44].

3. Results

(a) Aposymbiotic Aiptasia exhibit stronger transcriptomic responses to starvation than symbiotic Aiptasia

To compare the effect of starvation on gene expression in symbiotic and aposymbiotic Aiptasia, overall patterns of

gene expression were compared across treatment groups (Symbiotic Fed, Symbiotic Starved, Aposymbiotic Fed, and Aposymbiotic Starved) through PCA. PCA clustering showed that feeding status was a stronger predictor of gene expression (samples differentiated on PC1 explaining 30.8% of the variation) than symbiotic state (PC2 explaining 11.9% of the variation); however, both factors were significant ($p_{nut} < 0.001$; $p_{sym} = 0.017$; figure 1*b*). The interaction between feeding and symbiotic status was also significant ($p_{nut*sym} = 0.043$; figure 1*b*). Aposymbiotic Aiptasia exhibited stronger transcriptomic responses to starvation than symbiotic Aiptasia, as revealed by higher gene expression plasticity under starvation ($p < 0.001$; figure 1*c*). Under starvation, aposymbiotic Aiptasia had a greater number of DEGs (FDR-*p*-value of less than 0.05) than symbiotic anemones; that is, we identified 4858 starvation-induced DEGs in aposymbiotic compared to 1724 starvation-induced DEGs in symbiotic Aiptasia (figure 1*d*). A total of 1460 starvation-induced DEGs were shared between symbiotic and aposymbiotic Aiptasia, of which only 10 were expressed in opposite directions (electronic supplementary material, figure S1 and table S3), showing a similarity of starvation responses between symbiotic states. Lastly, from Fisher exact tests, Biological Process (BP) GO term enrichment of shared DEGs and symbiotic state-specific DEGs revealed enrichment of pathways involved in growth, metabolism, and response to oxidative stress (electronic supplementary material, dataset S2). This GO term pattern was exaggerated in aposymbiotic-unique DEGs; however, no clear functional differences across BP GO terms were observed between these categories (electronic supplementary material, dataset S2).

(b) Over-representation of immune pathways and under-representation of oxidative stress response pathways following starvation regardless of symbiotic state

To understand the functional drivers of the Aiptasia starvation response, we probed the over- and under-represented GO terms detected through BP GO term enrichment analysis of both symbiotic and aposymbiotic Aiptasia under starvation (electronic supplementary material, dataset S3). This analysis revealed strong signatures of enrichment for metabolism, immunity, and response to reactive oxygen species following starvation in both symbiotic and aposymbiotic states. GO terms associated with the innate immune system—specifically the NF-κB pathway (e.g. 'regulation of I-kappaB kinase/NF-kappaB signalling' GO:0043122)—were over-represented under starvation in both symbiotic and aposymbiotic conditions (electronic supplementary material, table S1). Additionally, general immune and stress response terms ('ROS response' hereafter; e.g. 'reactive oxygen species metabolic process' GO:0072593) were under-represented under starvation in both symbiotic and aposymbiotic conditions (electronic supplementary material, table S2).

From over-represented NF-κB pathway GO terms, we identified genes that were significantly upregulated under starvation in both symbiotic states, including two Tumor Necrosis Factor Receptor-Associated Factor homologues (TRAF4 and TRAF6) and a B-cell Lymphoma 3 (BCL3) homologue (figure 2*a*). Among the NF-κB pathway genes that were significantly upregulated under starvation only in aposymbiotic Aiptasia, we noted an additional BCL3 homologue, multiple homologues of NF-κB response genes (e.g. Tumor Necrosis Factor alpha-induced protein 3 (TNFAIP3)), and the NF-κB gene itself (figure 2*a*). However, a lesser number of NF-κB pathway genes were downregulated following starvation (e.g. CANT1).

From the under-represented GO terms associated with the ROS response, we identified genes that were significantly downregulated under starvation in both symbiotic and aposymbiotic Aiptasia, including four homologues for Superoxide Dismutase (SODA (a superoxide dismutase [Fe] homologue), SUPEROXIDE (a superoxide dismutase [Cu-Zn] homologue), SOD2 (a superoxide dismutase [Mn] homologue), and SOD (a putative superoxide dismutase [Cu-Zn] homologue)) (figure 2*b*). Among the oxidative stress response DEGs downregulated under starvation in aposymbiotic Aiptasia only, we identified an additional superoxide dismutase homologue (figure 2*b*). In aposymbiotic Aiptasia, some genes in the ROS Response pathway were upregulated following starvation (e.g. the Catalase homologue CAT).

(c) Starvation leads to upregulation of NF-κB protein and putative NF-κB target genes in both symbiotic and aposymbiotic Aiptasia

Because NF-κB pathway GO terms and associated genes were enriched in starved Aiptasia, we sought to determine whether NF-κB protein levels were higher in starved anemones relative to fed ones. By Western blotting, we compared NF-κB protein levels in clonal pairs of fed and starved symbiotic and aposymbiotic Aiptasia. Levels of the processed (active) form of NF-κB protein were approximately 2.8 times higher in starved compared to fed symbiotic Aiptasia, and approximately 2.5 times higher in starved compared to fed aposymbiotic Aiptasia (figure 3*a*).

To further explore upregulation of the NF-κB pathway following starvation in symbiotic and aposymbiotic Aiptasia, we identified significantly upregulated genes under starvation (FDR-*p*-value of less than 0.05) that were previously shown to be heat responsive and to contain at least three NF-κB binding sites in the region 500 bp upstream of the transcription start site (electronic supplementary material, tables S5 and S6) [39]. In starved symbiotic and aposymbiotic Aiptasia, significantly upregulated putative NF-κB target genes included BCL3 and other genes implicated in innate immunity (e.g. Interferon-induced helicase C domain-containing protein 1 (IFIH1) and Guanylate-binding protein 5 (GBP5); figure 3*b*). Starved aposymbiotic Aiptasia showed upregulation of several additional putative NF-κB target genes, including NF-κB itself (figure 3*b*).

(d) Pathogen and ROS susceptibility is variable across symbiotic and nutritional states

To determine whether the observed differential regulation of the immune and oxidative stress responses following starvation leads to altered susceptibility to immune and oxidative challenges, we performed pathogen and ROS exposure experiments. We found that anemones exposed to four weeks of the bacterial pathogens Pa14 or Smarc showed differential mortality across symbiotic states and feeding status. Symbiotic Fed (SymFed) Aiptasia exposed to Pa14 had higher risk of mortality than Symbiotic Starved (SymStarved) Aiptasia (Bonferroni-adjusted *p*-value < 0.001) (figure 4*a*). SymFed Aiptasia also showed higher mortality when exposed to Smarc than SymStarved anemones (Bonferroni-adjusted *p*-value < 0.001)

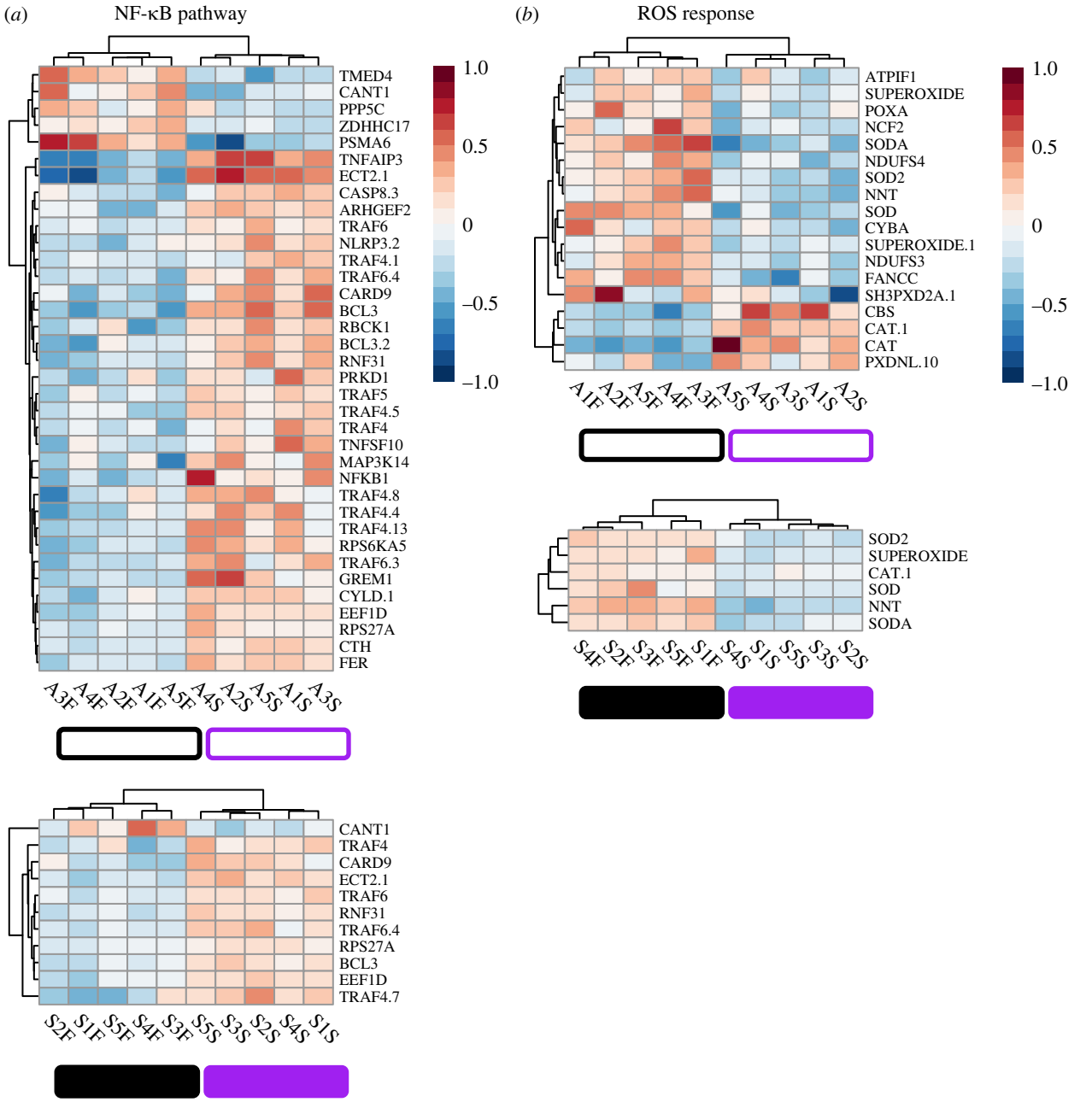

Figure 2. Differential regulation of NF-κB and ROS stress responses under starvation in Aiptasia. (*a*) Significantly differentially expressed genes (DEGs) (FDR-adjusted-*p* value < 0.05) in the NF-κB pathway (aposymbiotic clonal pairs top, symbiotic clonal pairs bottom). (*b*) Significantly DEGs involved in the response to reactive oxygen species (ROS; aposymbiotic clonal pairs top, symbiotic clonal pairs bottom). Colour scale of heatmaps represents the $\log_2$ fold change of each gene (row) for each anemone (column) relative to the gene's mean across all anemones. Dendrograms are hierarchical clustering of genes based on similarity of expression across samples. In both panels, aposymbiotic anemones are represented by open boxes and symbiotic anemones are represented by closed boxes. Purple indicates starved samples and black indicates fed samples. Full gene names and annotations are included in electronic supplementary material table S4.

(figure 4*b*). Additionally, Aposymbiotic Starved (ApoStarved) Aiptasia had a higher risk of mortality than SymStarved Aiptasia following exposure to both pathogens (Bonferroni-adjusted *p*-value < 0.001) (figure 4*a*,*b*). However, in both pathogen challenges, starvation increased susceptibility to bacteria in aposymbiotic Aiptasia, as observed by the higher risk of mortality in ApoStarved compared to Aposymbiotic Fed (ApoFed) Aiptasia (Bonferroni-adjusted *p*-value < 0.001 for Pa14, Bonferroni-adjusted *p*-value < 0.05 for Smarc) (figure 4*a*,*b*). Finally, ApoFed had a consistently lower risk of mortality than SymFed following exposure to Pa14 (Bonferroni-adjusted *p*-value < 0.01) and Smarc (Bonferroni-adjusted *p*-value < 0.001) (figure 4*a*,*b*). Overall, these results demonstrate that starvation is protective against pathogen-induced mortality in symbiotic, but not aposymbiotic, Aiptasia.

When exposed to four weeks of 0.008% H_2O_2, both symbiotic and aposymbiotic anemones showed lower survival probabilities when starved as compared to fed Aiptasia exposed to H_2O_2 (Bonferroni-adjusted *p*-value < 0.001 for aposymbiotic and symbiotic) (figure 4*c*).

(e) Among different cnidarians, starvation leads to similar changes in gene expression related to metabolism and oxidative stress, but not the immune response

We performed a meta-analysis using previously published starvation-based gene expression datasets to determine the degree of similarity in transcriptomic responses to starvation

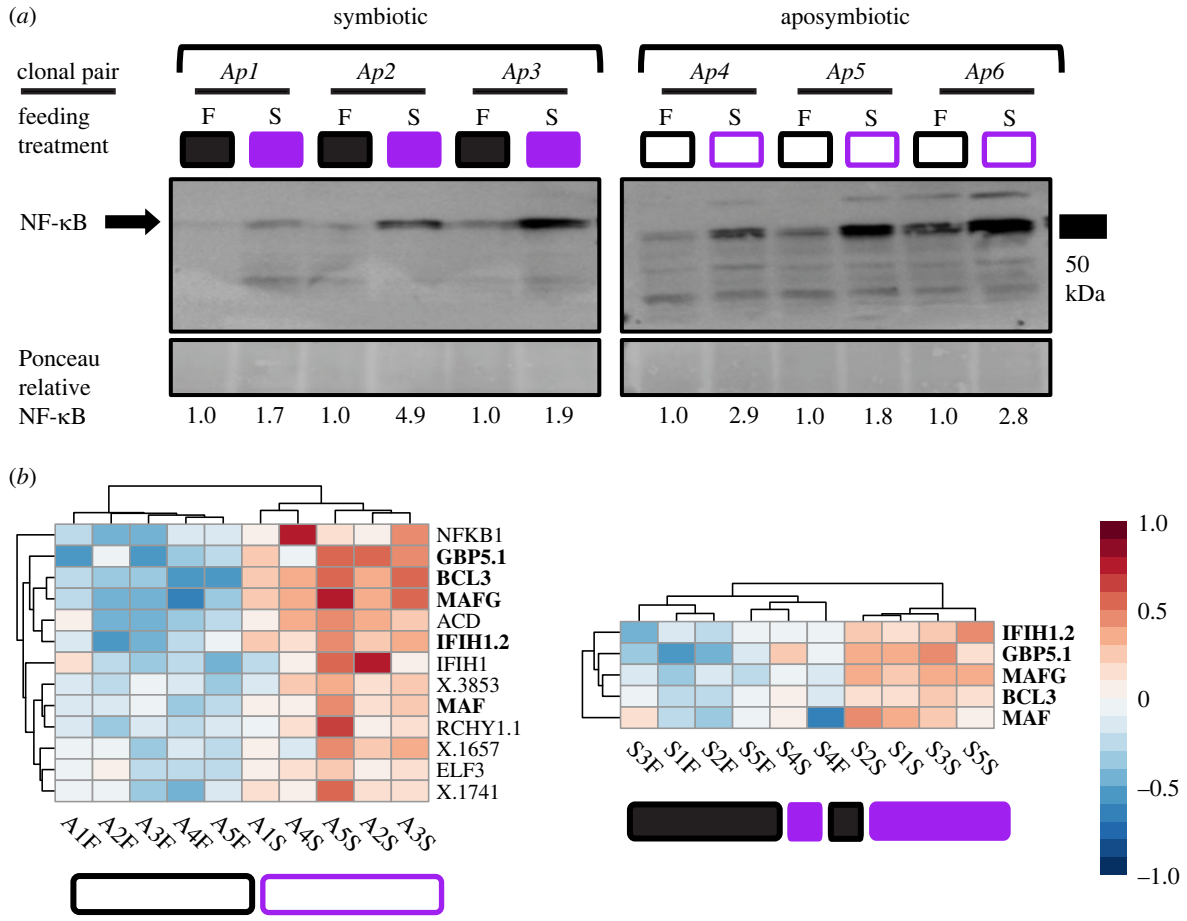

Figure 3. Upregulation of the NF-κB protein and putative NF-κB target genes under starvation in Aiptasia. (*a*) Western blot of NF-κB in symbiotic (left) and aposymbiotic (right) clonal pairs (Ap1-6) under fed (F) or starved (S) conditions. NF-κB protein levels were normalized to Ponceau staining. Values below blots are normalized NF-κB levels relative to fed Aiptasia of each clonal pair (1.0) (e.g. F1/F1 and S1/F1 for Ap1). Location of the 50 kDa molecular weight marker is indicated to the right of the blots. (*b*) Significantly upregulated (FDR *p*-value < 0.05) heat-responsive genes previously characterized as putative NF-κB target genes [45] in aposymbiotic (left) and symbiotic clonal pairs (right). These genes have three or more NF-κB binding sites in the region 500 bp upstream of the transcription start site [45] (electronic supplementary material table S5 and table S6). Bolded genes are shared between aposymbiotic and symbiotic states. The gene 'ACD' was shortened from 'ACD_16C00100G0095'. Full gene names and annotations are included in electronic supplementary material table S4. Heatmap colour scale represents the $\log_2$ fold change of each gene (row) for each anemone (column) relative to the gene's mean across all anemones. Dendrograms are hierarchical clustering of genes based on similarity of expression across samples. In both panels, aposymbiotic anemones are represented by open boxes and symbiotic anemones are represented by closed boxes. Purple indicates starved samples and black indicates fed samples.

among different cnidarians. In symbiotic and aposymbiotic Aiptasia, non-symbiotic *N. vectensis*, and symbiotic *O. arbuscula*, we observed downregulation of metabolic processes following starvation (electronic supplementary material, figure S2). By comparing the delta rank values of all BP GO terms that were over- or under-represented (FDR-*p*-value of less than 0.1) following starvation in at least two taxa, there was extensive downregulation of terms associated with biosynthetic (e.g. 'carbohydrate biosynthetic process' GO:0016051), metabolic (e.g. 'carbohydrate metabolic process' GO:0005975), and catabolic (e.g. 'carbohydrate catabolic process' GO:0016052) processes. These results indicate that starvation restricts energetic supply to cause gene expression changes across different experiments, species, and symbiotic states (figure 5*a*).

GO enrichment analysis of starvation in symbiotic and aposymbiotic Aiptasia showed clear enrichment of immunity, stress, and defence (electronic supplementary material, tables S1 and S2). To determine if these patterns were also observed in other cnidarians, we extracted enriched GO terms (FDR-*p*-value < 0.1) associated with immunity, stress, and defence from starvation experiments in *N. vectensis* and *O. arbuscula* (electronic supplementary material, figure S2). We found that many terms associated with broad immune system processes (e.g. 'regulation of immune system process' GO:0002684 and 'defence response' GO:0006952) were enriched in the opposite direction in non-symbiotic *N. vectensis* compared to species capable of symbiosis (Aiptasia and *O. arbuscula*). In particular, the GO term 'Immune Response' (GO:0006955) was over-represented under starvation conditions in symbiotic Aiptasia, aposymbiotic Aiptasia, and symbiotic *O. arbuscula*, but was under-represented in starved *N. vectensis*. However, GO terms associated with the oxidative stress response pathway ('reactive oxygen species metabolic process' GO:0072593) were under-represented in starved *N. vectensis* along with starved symbiotic and aposymbiotic Aiptasia (these terms were not significant in *O. arbuscula*) (figure 5*b*). Overall, stress response pathways associated with ROS were downregulated under starvation across taxa, whereas cnidarians capable of symbiosis consistently upregulated immune system pathways under starvation.

4. Discussion

Here, we describe the effects of starvation on gene expression, immunity, and oxidative stress responses in symbiotic and

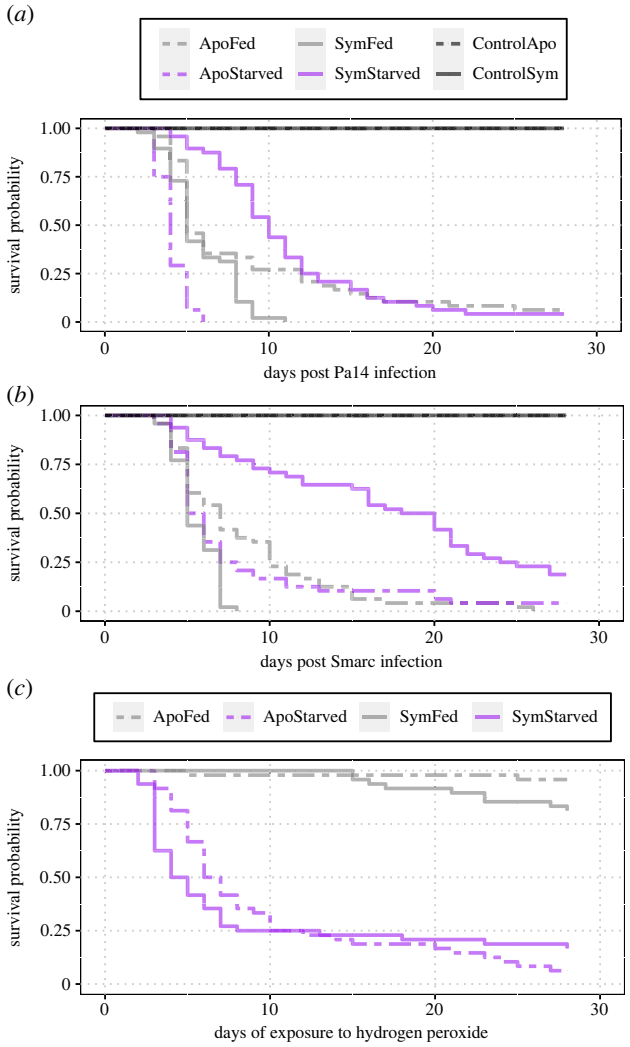

Figure 4. Starvation affects susceptibility to pathogen and oxidative stress in Aiptasia. Survival curves in fed and starved symbiotic and aposymbiotic Aiptasia exposed to 28 days of control conditions or a 28-day pathogen challenge with *Pseudomonas aeruginosa* (Pa14) (*a*) or *Serratia marcescens* (Smarc) (*b*). No mortality was observed in control conditions in either (*a*) or (*b*) challenge experiments. (*c*) Survival curves in fed and starved symbiotic and aposymbiotic Aiptasia exposed to 28 days of 0.008% H_2O_2.

aposymbiotic anemones of the cnidarian model Aiptasia. We identified a core set of genes whose expression changes in response to starvation in both symbiotic and aposymbiotic anemones; however, there are also many gene expression changes that are unique to aposymbiotic anemones. Across symbiotic states, starvation induces expression of the NF-κB transcription factor, as well as genes associated with the NF-κB pathway; however, starvation-induced upregulation of NF-κB is not necessarily predictive of organismal susceptibility to pathogen-induced mortality. Furthermore, pathogen-specific immunity appears to be regulated independently from the oxidative stress response, suggesting that these two 'defence' responses have distinct energetic priorities under conditions in which heterotrophy-derived nutrients are limited. Finally, a meta-analysis comparing gene expression responses to starvation across cnidarian taxa showed that cnidarian species—including Aiptasia, the non-symbiotic anemone *N. vectensis*, and the facultatively symbiotic coral *O. arbuscula*—vary in how they respond to starvation, suggesting that starvation-induced gene expression and pathway responses are modulated by the animal's ability to undergo symbiosis with Symbiodiniaceae algae.

One striking feature of our study was the strength of transcriptomic responses to starvation that occurred in aposymbiotic Aiptasia as compared to symbiotic Aiptasia. Starvation resulted in approximately three times as many DEGs in aposymbiotic anemones as compared to symbiotic anemones (4858 versus 1724), with aposymbiotic Aiptasia modulating 18% of its genes under starvation (4858 of approx. 27 000). Although starvation was a stronger predictor of overall transcriptomic profiles than symbiotic state (drove variation along PC1 that explained 30.8% of gene expression variation; high number of shared DEGs (1460) across both symbiotic and aposymbiotic anemones), there were 3400 starvation-induced DEGs that were unique to aposymbiotic Aiptasia, as compared to only 256 DEGs unique to symbiotic anemones. Pathway analysis of shared DEGs between aposymbiotic and symbiotic anemones under starvation revealed enrichment of processes involved in regulating growth, metabolism, and response to stress; however, these pathways were more highly enriched in aposymbiotic-specific DEGs. These analyses reveal that the overall regulatory processes that are rewired under conditions of food deprivation are similar between symbiotic states.

The stronger effects of starvation on gene expression in aposymbiotic Aiptasia are likely because starved symbiotic Aiptasia can still obtain sufficient energy from the carbon translocated from their algal symbionts [45]. Therefore, symbiotic Aiptasia may be buffered from the effects of starvation by symbiont-derived energy sources. However, starved symbiotic Aiptasia still experience nutrition stress, as demonstrated by the 1724 DEGs and differentially regulated metabolism and growth gene pathways under starvation, possibly driven by a lack of nitrogen and other essential nutrients typically derived from heterotrophic sources [45]. These results suggest that energetic reserves, whether from symbiotic or heterotrophic sources, provide a mechanism for protection against environmental stress. Indeed, previous research showed that corals that can compensate for the loss of symbiont-derived nutrients with heterotrophy are more resilient to heat-induced bleaching [8,10]. As such, under starvation, cnidarians must restructure their gene expression profiles to optimize energy use and prioritize gene pathways that promote survival.

Starvation also led to increased NF-κB protein levels, as well as enrichment of NF-κB-related GO terms, associated pathway genes (e.g. TRAF4, TRAF6, and TNFAIP3), and possible target genes (e.g. BCL3, and GBP5), in both symbiotic and aposymbiotic Aiptasia. NF-κB protein levels increased in starved symbiotic (2.8-fold increase) and aposymbiotic (2.5-fold increase) Aiptasia, which is in contrast to non-symbiotic *N. vectensis*, where starvation led to a 20% reduction in NF-κB protein levels and downregulation of associated gene expression pathways [12]. Decreased NF-κB protein in *N. vectensis* was also correlated with increased susceptibility to bacteria-induced mortality [12]. Although our experiments showed starvation-induced increases in NF-κB were correlated with decreased susceptibility to bacterial mortality in symbiotic Aiptasia, that was not the case with aposymbiotic Aiptasia, where starvation led to increased NF-κB protein and increased susceptibility to bacteria-induced mortality. Therefore, NF-κB is not the sole molecular inducer of immunity in Aiptasia, and NF-κB may have roles in addition to pathogen immunity in this species. We previously showed that heat- or menthol-induced loss of symbionts in Aiptasia leads to increased levels of NF-κB [18], suggesting that

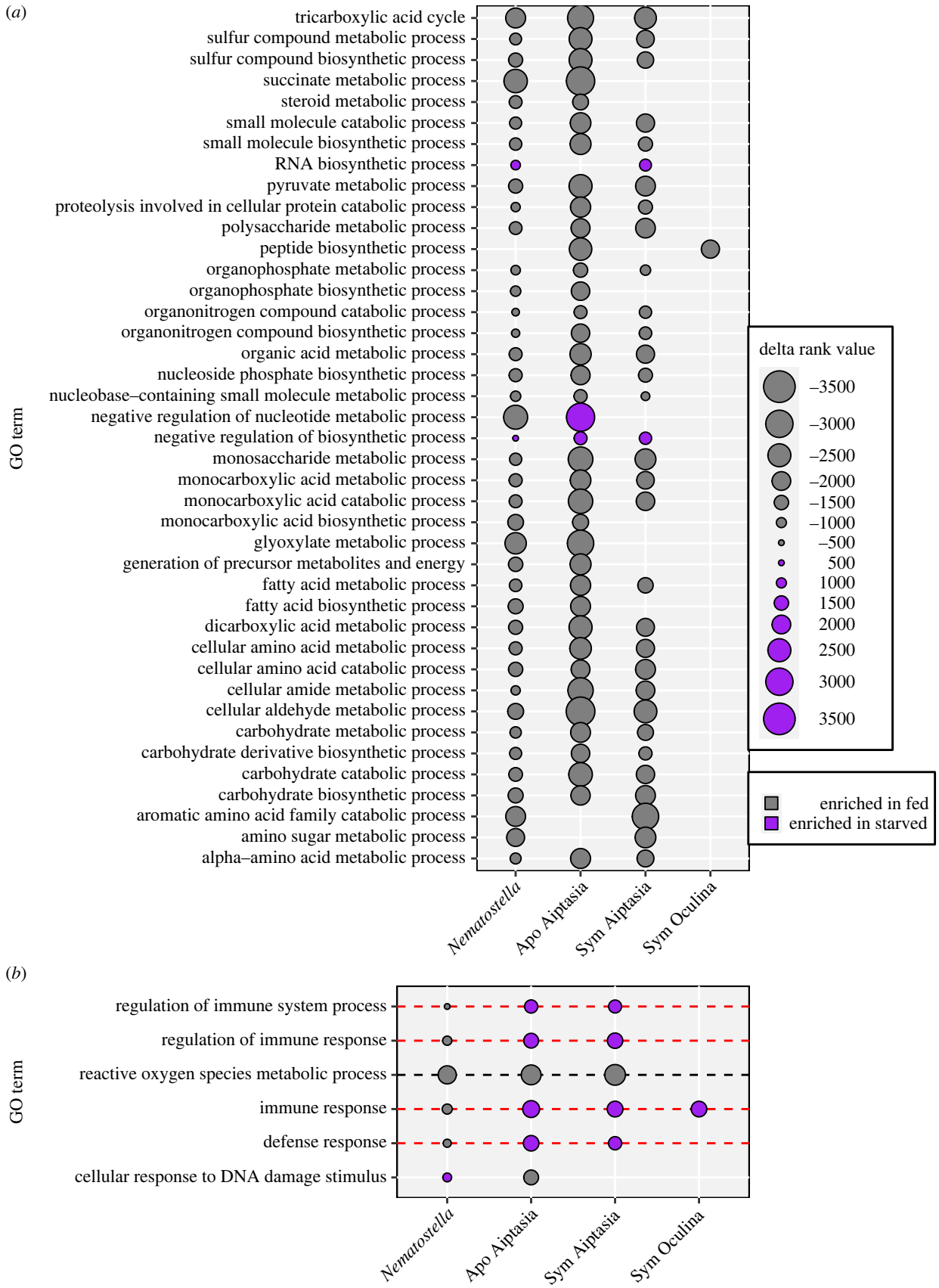

Figure 5. Gene Ontology (GO) term comparisons confirm nutrient limitation and reveal divergent regulation of immune and stress response pathways across Cnidaria. Delta rank values (represented by point size) were compared across starvation experiments in *Nematostella vectensis* (*Nematostella* [12]), aposymbiotic (Apo, this study) Aiptasia, symbiotic (Sym, this study) Aiptasia, and symbiotic *Oculina arbtauscula* (Sym Oculina [7]). Terms were plotted if they were significantly enriched in fed (grey, negative delta rank values) or starved (purple, positive delta rank values) treatments in at least two comparisons. GO terms enriched in aposymbiotic and symbiotic Aiptasia, but in neither of the other species, were not included. (*a*) Shared GO terms corresponding to metabolism, catabolism, and biosynthesis were plotted to demonstrate conserved downregulation under starvation across cnidarian taxa. (*b*) Shared GO terms corresponding to immunity, stress, and defence were plotted to demonstrate differences in regulation of these pathways in *Nematostella* compared to Aiptasia and Oculina. Bold GO groups are those that are significantly enriched under starvation (either positively or negatively) in at least three systems. Red, dashed lines indicate GO groups enriched in the opposite direction in *Nematostella* compared to at least two of the three other systems. Black, dashed lines indicate GO groups enriched in the same direction in at least three systems.

algal symbionts suppress NF-κB activity to aide in establishment of symbiosis. Furthermore, NF-κB and several putative NF-κB-responsive genes are rapidly, albeit transiently, induced by heat shock in Aiptasia [39]. Of note, we found many of the same heat shock-induced genes with multiple upstream NF-κB sites are also induced by starvation in Aiptasia. However, it has not been determined whether the genes shown in figure 3*b* are direct target genes of Ap-NF-κB, nor have roles been determined for NF-κB or its target genes in the regulation of symbiosis, the response to heat shock, or starvation-induced biological responses.

Overall, evidence suggests that NF-κB has different roles in Aiptasia and *N. vectensis*. Like Aiptasia, the facultatively symbiotic coral *O. arbuscula* shows an upregulation of immune response pathways under starvation. Moreover, thermal challenges have been shown to upregulate NF-κB transcripts in symbiotic anemones [39,46] and in multiple species of symbiotic coral [47,48]. Thus, it appears that NF-κB has different roles in cnidarians existing with versus without symbionts. Increased expression of NF-κB protein and possible NF-κB target genes following both heat shock and starvation strengthens the argument for a role of this transcription factor pathway in affecting symbiont cell density under conditions that are unfavourable for symbiosis, such as heterotrophy-limited conditions [16]. We hypothesize that the mechanism by which starvation induces NF-κB in Aiptasia is due to a switch of the symbiosis from a mutualism to a parasitism as nutrients become limiting. Although we did not demonstrate that symbiont cell density is more tightly regulated under starvation, this switch has been proposed under thermal stress in symbiotic coral, wherein nutrient exchange becomes decoupled due to the symbionts sequestering resources from the coral host [10,49]. In symbiotic Aiptasia under starvation, a similar nutrient sequestration by the symbiont may occur, leading to a bleaching phenotype via induction of the symbiont-regulatory NF-κB pathway. In aposymbiotic Aiptasia under starvation where there are no symbionts to sequester nutrients, NF-κB pathway induction may be programmed to occur when nutrients are scarce. However, NF-κB induction is not just subsequent to starvation-induced symbiont loss, as NF-κB increased in starved aposymbiotic and symbiotic Aiptasia. As such, future work should explore interactions between starvation, symbiont density, and symbiont health, and how these interactions cause NF-κB activation. Our data indicate that NF-κB is activated transcriptionally in Aiptasia (as evidenced by increased NF-κB expression in starved aposymbiotic Aiptasia), rather than primarily through protein modification, as occurs in mammals. Our research contributes to the understanding of NF-κB biology beyond immunity to pathogens, as has been seen in the ability of NF-κB to control early developmental processes in *Drosophila* [50] and *N. vectensis* [51].

In contrast to pathogen responses, starvation leads to increased susceptibility to oxidative stress and downregulation of oxidative stress response genes in both symbiotic and aposymbiotic Aiptasia. For example, four SOD homologues were downregulated under starvation in Aiptasia from both states and an additional SOD homologue was downregulated in aposymbiotic Aiptasia only. SODs are involved in quenching ROS that increase in concentration under stress, thus ameliorating cell damage [52]. Increased SOD expression has been documented under various stress conditions in Aiptasia both in and out of symbiosis [28,53] as well as in multiple species of coral [54]. While most oxidative stress response genes were downregulated under starvation in aposymbiotic Aiptasia, some oxidative stress response genes (CBS, CAT, CAT.1, and PXDNL.10) were upregulated. These nuanced responses within the oxidative stress-related pathway highlight their molecular complexity and limitations in our knowledge of gene function in basal metazoans. Overall, these results demonstrate that, unlike the NF-κB pathway, energy is directed away from the ROS response under starvation, suggesting that the response to oxidative stress is not an energetic priority for Aiptasia under nutrient limitation.

The analysis of shared GO terms across three starved cnidarian species showcased differences in expression of immune and oxidative stress terms according to the organism's capacity for symbiosis. Although oxidative stress terms were overall under-represented following starvation across all taxa, immune terms showed variation: they were over-represented following starvation in Aiptasia and *O. arbuscula* (both facultatively symbiotic species), while they were under-represented in starved non-symbiotic *N. vectensis*. These results suggest that a cnidarian's capacity for symbiosis causes distinct energetic priorities and regulatory pathways within 'defence' responses. These results highlight the need for caution when applying broad categorization of gene expression pathways that were described in other, evolutionarily distinct species, which may have evolutionarily distinct immune and stress regulatory pathways.

Altogether, cnidarian responses to pathogen or stress challenges are dependent on multiple factors, including symbiotic state, symbiotic capacity, and nutrition levels, which should be considered when predicting how cnidarians will respond to perturbation. Unique energetic priorities were observed between oxidative stress (low priority), symbiont-regulatory immunity (high priority), and pathogen immunity (dependent on symbiosis and/or heterotrophy) within the cnidarian 'defence' response. The dependence of pathogen immunity on both symbiotic status and nutritional state may explain the contrasting effects of bleaching on pathogen immunity observed in the field where some data demonstrate that bleaching increases resistance to disease [20], while other data suggest that bleaching increases susceptibility to disease [55]. These contradictions may be explained by the bleached animal's capacity to supplement its energetic needs with heterotrophy [20,56,57]. Our findings contribute to the growing literature exploring the diverse biological processes (e.g. immunity, development and symbiosis) impacted by NF-κB in basal metazoans [12,18,51,58]. The implications of these results are three-fold: (1) NF-κB and NF-κB gene pathways are either independent from Aiptasia pathogen-linked immunity, or they are not sufficient to defend against pathogen-induced mortality in the absence of adequate energetic reserves; (2) the oxidative stress response is dependent upon the availability of accessible nutrients beyond simple sugars; and (3) the oxidative stress response and the immune response have distinct energetic priorities in Aiptasia.

Although we did not explore the interaction between inorganic and organic nutrient sources, previous research suggests that increased concentrations of inorganic compounds from anthropogenic sources compared to organic, bioavailable nutrient forms hinder photosynthesis and can disrupt nutrient exchange between endosymbionts and cnidarian hosts [9,59]. Furthermore, coral bleaching results in starvation when hosts cannot effectively counterbalance

nutrient loss with heterotrophy [60]. Taken together, it is clear that proper nutrient availability and acquisition from various sources can significantly impact an organism's capacity to withstand stressors. Thus, it is important to understand the molecular and physiological responses of cnidarians under conditions of differing nutrient availability and how these responses vary by species, symbiotic states and symbiotic capacities.

Ethics. This work did not require ethical approval from a human subject or animal welfare committee.

Data accessibility. Raw fastq files for all gene expression samples are publicly available here: SRA BioProject PRJNA987812. All data and code can be found here: https://github.com/mariaingersoll/Aiptasia_Fed_Starved/tree/48dd41d8c31a2c250dc45c5fbaba5f3333213060.

Supplementary material is available online [61].

Declaration of AI use. We have not used AI-assisted technologies in creating this article.

Authors' contributions. M.V.-I.: conceptualization, data curation, formal analysis, investigation, methodology, visualization, writing—original draft, writing—review and editing; P.J.A.C.: conceptualization, investigation, methodology, writing—review and editing; C.A.B.: investigation, methodology, writing—review and editing; N.A.D.: investigation, methodology, writing—review and editing; T.D.G.: conceptualization, funding acquisition, investigation, methodology, project administration, resources, supervision, writing—original draft, writing—review and editing; S.W.D.: conceptualization, funding acquisition, investigation, methodology, project administration, supervision, writing—original draft, writing—review and editing.

All authors gave final approval for publication and agreed to be held accountable for the work performed therein.

Conflict of interest declaration. We declare we have no competing interests.

Funding. This research was supported by National Science Foundation grant IOS-1937650 (to T.D.G. and S.W.D.). M.V.-I. was supported by an NSF Graduate Research Fellowship and NSF NRT DGE 1735087. P.J.A.C. was supported by a Warren McLeod Marine Fellowship. C.A.B. and N.A.D. were supported by the Boston University Undergraduate Research Opportunities Program, and N.A.D. received support from New England Biolabs and Dr Loren Wold.

Acknowledgements. We thank Stephen Lory (Harvard University) for *Pseudomonas aeruginosa* strain Pa14 and Kim Ritchie (University of South Carolina Beaufort) for *Serratia marcescens*. We also thank Nils Rädecker and the anonymous reviewer for their insight.

References

1. Puntin G, Sweet M, Fraune S, Medina M, Sharp K, Weis VM, Ziegler M. 2022 Harnessing the power of model organisms to unravel microbial functions in the coral holobiont. *Microbiol. Mol. Biol. Rev.* **86**, e0005322. (doi:10.1128/mmbr.00053-22)
2. Muscatine L, Porter JW. 1977 Reef corals: mutualistic symbioses adapted to nutrient-poor environments. *BioScience* **27**, 454–460. (doi:10.2307/1297526)
3. Lipschultz F, Cook C. 2002 Uptake and assimilation of ^{15}N-ammonium by the symbiotic sea anemones *Bartholomea annulata* and *Aiptasia pallida*: conservation versus recycling of nitrogen. *Mar. Biol.* **140**, 489–502. (doi:10.1007/s00227-001-0717-1)
4. Muscatine L, Cernichiari E. 1969 Assimilation of photosynthetic products of zooxanthellae by a reef coral. *Biol. Bull.* **137**, 506–523. (doi:10.2307/1540172)
5. Hoegh-Guldberg O. 2010 Coral reef ecosystems and anthropogenic climate change. *Reg. Environ. Change* **11**, 215–227. (doi:10.1007/s10113-010-0189-2)
6. Aichelman HE, Townsend JE, Courtney TA, Baumann JH, Davies SW, Castillo KD. 2016 Heterotrophy mitigates the response of the temperate coral *Oculina arbuscula* to temperature stress. *Ecol. Evol.* **6**, 6758–6769. (doi:10.1002/ece3.2399)
7. Rivera HE, Tramonte CA, Samaroo J, Dickerson H, Davies SW. 2023 Heat challenge elicits stronger physiological and gene expression responses than starvation in symbiotic *Oculina arbuscula*. *J.Hered.* **114**, 312–325. (doi:10.1093/jhered/esac068)
8. Grottoli A, Rodrigues L, Palardy J. 2006 Heterotrophic plasticity and resilience in bleached corals. *Nature* **440**, 1186–1189. (doi:10.1038/nature04565)
9. Morris LA, Voolstra CR, Quigley KM, Bourne DG, Bay LK. 2019 Nutrient availability and metabolism affect the stability of coral–Symbiodiniaceae symbioses. *Trends Microbiol.* **27**, 678–689. (doi:10.1016/j.tim.2019.03.004)
10. Sangmanee K, Casareto BE, Nguyen TD, Sangsawang L, Toyoda K, Suzuki T, Suzuki Y. 2020 Influence of thermal stress and bleaching on heterotrophic feeding of two scleractinian corals on pico-nanoplankton. *Mar. Pollut. Bull.* **158**, 111405. (doi:10.1016/j.marpolbul.2020.111405)
11. Gault JA, Bentlage B, Huang D, Kerr AM. 2021 Lineage-specific variation in the evolutionary stability of coral photosymbiosis. *Sci. Adv.* **7**, eabh4243. (doi:10.1126/sciadv.abh4243)
12. Aguirre Carrión PJ, Desai N, Brennan JJ, Fifer J, Siggers T, Davies SW, Gilmore TD. 2023 Starvation decreases immunity and immune regulatory factor NF-κB in the starlet sea anemone *Nematostella vectensis*. *Commun. Biol.* **6**, 698. (doi:10.1038/s42003-023-05084-7)
13. Rädecker N, Raina J-B, Pernice M, Perna G, Guagliardo P, Kilburn MR, Aranda M, Voolstra CR. 2018 Using Aiptasia as a model to study metabolic interactions in cnidarian-*Symbiodinium* symbioses. *Front. Physiol.* **9**, 214. (doi:10.3389/fphys.2018.00214)
14. Weis VM. 2008 Cellular mechanisms of Cnidarian bleaching: stress causes the collapse of symbiosis. *J. Exp. Biol.* **211**, 3059–3066. (doi:10.1242/jeb.009597)
15. Davy SK, Allemand D, Weis VM. 2012 Cell biology of cnidarian-dinoflagellate symbiosis. *Microbiol. Mol. Biol. Rev.* **76**, 229–261. (doi:10.1128/MMBR.05014-11)
16. Davy S, Cook C. 2001 The relationship between nutritional status and carbon flux in the zooxanthellate sea anemone *Aiptasia pallida*. *Mar. Biol.* **139**, 999–1005. (doi:10.1007/s002270100640)
17. Rossett SL, Oakley CA, Ferrier-Pages C, Suggett DJ, Weis VM, Davy SK. 2021 The molecular language of the cnidarian-dinoflagellate symbiosis. *Trends Microbiol.* **29**, 320–333. (doi:10.1016/j.tim.2020.08.005)
18. Mansfield KM *et al.* 2017 Transcription factor NF-κB is modulated by symbiotic status in a sea anemone model of cnidarian bleaching. *Sci. Rep.* **7**, 16025. (doi:10.1038/s41598-017-16168-w)
19. Rivera HE, Davies SW. 2021 Symbiosis maintenance in the facultative coral, *Oculina arbuscula*, relies on nitrogen cycling, cell cycle modulation, and immunity. *Sci. Rep.* **11**, 21226. (doi:10.1038/s41598-021-00697-6)
20. Merselis DG, Lirman D, Rodriguez-Lanetty M. 2018 Symbiotic immuno-suppression: is disease susceptibility the price of bleaching resistance? *PeerJ* **6**, e4494. (doi:10.7717/peerj.4494)
21. Changsut I, Womack HR, Shickle A, Sharp KH, Fuess LE. 2022 Variation in symbiont density is linked to changes in constitutive immunity in the facultatively symbiotic coral, *Astrangia poculata*. *Biol. Lett.* **18**, 20220273. (doi:10.1098/rsbl.2022.0273)
22. Cotinat P, Fricano C, Toullec G, Röttinger E, Barnay-Verdier S, Furla P. 2022 Intrinsically high capacity of animal cells from a symbiotic cnidarian to deal with pro-oxidative conditions. *Front. Physiol.* **13**, 819111. (doi:10.3389/fphys.2022.819111)
23. Langmead B, Salzberg S. 2012 Fast gapped-read alignment with Bowtie 2. *Nat. Methods* **9**, 357–359. (doi:10.1038/nmeth.1923)
24. Sunagawa S, Wilson EC, Thaler M, Smith ML, Caruso C, Pringle JR, Weis VM, Medina M, Schwarz JA. 2009 Generation and analysis of transcriptomic resources for a model system on the rise: the sea anemone *Aiptasia pallida* and its dinoflagellate endosymbiont. *BMC Genom.* **10**, 258. (doi:10.1186/1471-2164-10-258)
25. Dani V, Priouzeau F, Pagnotta S, Carette D, Laugier JP, Sabourault C. 2016 Thermal and menthol stress

induce different cellular events during sea anemone bleaching. *Symbiosis* **69**, 175–192. (doi:10.1007/s13199-016-0406-y)

26. Hannon GJ. 2010 FASTX-Toolkit. See http://hannonlab.cshl.edu/fastx_toolkit.
27. Baumgarten S *et al.* 2015 The genome of Aiptasia, a sea anemone model for coral symbiosis. *Proc. Natl Acad. Sci. USA* **112**, 11 893–11 898. (doi:10.1073/pnas.1513318112)
28. González-Pech RA *et al.* 2021 Comparison of 15 dinoflagellate genomes reveals extensive sequence and structural divergence in family Symbiodiniaceae and genus Symbiodinium. *BMC Biology* **19**, 661. (doi:10.1186/s12915-021-00994-6)
29. R Core Team. 2023 *R: a language and environment for statistical computing*. Vienna, Austria: R Foundation for Statistical Computing.
30. Love MI, Huber W, Anders S. 2014 Moderated estimation of fold change and dispersion for RNA-seq data with DESeq2. *Genome Biol.* **15**, 550. (doi:10.1186/s13059-014-0550-8)
31. Kauffmann A, Gentleman R, Huber W. 2009 arrayQualityMetrics: a bioconductor package for quality assessment of microarray data. *Bioinformatics* **25**, 415–416. (doi:10.1093/bioinformatics/btn647)
32. Oksanen J *et al*. 2022 vegan: community ecology package. R package version 2.6-4.
33. Martinez Arbizu P. 2020 pairwiseAdonis: pairwise multilevel comparison using Adonis. R package version 0.4.
34. Bove C. 2022 RandomFun: plasticity from PC distances (Version 1.0) [Computer software].
35. Bove CB, Davies SW, Ries JB, Umbanhowar J, Thomasson BC, Farquhar EB, McCoppin JA, Castillo KD. 2022 Global change differentially modulates Caribbean coral physiology. *PLoS ONE* **17**, e0273897.
36. Chen H. 2022 VennDiagram: generate high-resolution Venn and Euler plots. R package version 1.7.3. See https://CRAN.R-project.org/package=VennDiagram.
37. Wright RM, Aglyamova GV, Meye E, Matz MV. 2015 Gene expression associated with white syndromes in a reef building coral, *Acropora hyacinthus*. *BMC Genom.* **16**, 371. (doi:10.1186/s12864-015-1540-2)
38. Kolde R. 2019 pheatmap: pretty heatmaps. R package version 1.0.12. See https://CRAN.R-project.org/package=pheatmap.
39. Cleves PA, Krediet CJ, Lehnert EM, Onishi M, Pringle JR. 2020 Insights into coral bleaching under heat stress from analysis of gene expression in a sea anemone model system. *Proc. Natl. Acad. Sci. USA* **117**, 28 906–28 917. (doi:10.1073/pnas.2015737117)
40. Friedman LE, Gilmore TD, Finnerty JR. 2018 Intraspecific variation in oxidative stress tolerance in a model cnidarian: differences in peroxide sensitivity between and within populations of *Nematostella vectensis*. *PLoS ONE* **13**, e0188265.
41. Therneau T. 2023 A package for survival analysis in R. R package version 3.5-5. See https://CRAN.R-project.org/package=survival.
42. Therneau TM, Grambsch PM. 2000 *Modeling survival data: extending the Cox model*. New York, NY: Springer.
43. Kassambara A, Kosinski M, Biecek P. 2021 survminer: drawing survival curves using 'ggplot2'. R package version 0.4.9. See https://CRAN.R-project.org/package=survminer.
44. Wickham H. 2016 *Ggplot2: elegant graphics for data analysis*. New York, NY: Springer-Verlag.
45. Rädecker N, Meibom A. 2023 Symbiotic nutrient cycling enables the long-term survival of Aiptasia in the absence of heterotrophic food sources. *Peer Community J* **3**, e48. (doi:10.24072/pcjournal.281)
46. Eliachar S *et al.* 2022 Heat stress increases immune cell function in Hexacorallia. *Front. Immunol.* **13**, 1016097. (doi:10.3389/fimmu.2022.1016097)
47. Traylor-Knowles N, Rose NH, Sheets EA, Palumbi SR. 2017 Early transcriptional responses during heat stress in the coral *Acropora hyacinthus*. *Biol. Bull.* **232**, 91–100. (doi:10.1086/692717)
48. Majerova E, Carey FC, Drury C, Gates RD. 2021 Preconditioning improves bleaching tolerance in the reef-building coral *Pocillopora acuta* through modulations in the programmed cell death pathways. *Mol. Ecol.* **30**, 3560–3574. (doi:10.1111/mec.15988)
49. Baker DM, Freeman CJ, Wong JCY, Fogel ML, Knowlton N. 2018 Climate change promotes parasitism in a coral symbiosis. *ISME, J.* **12**, 921–930. (doi:10.1038/s41396-018-0046-8)
50. Steward R. 1987 Dorsal, an embryonic polarity gene in *Drosophila*, is homologous to the vertebrate proto-oncogene, c-*rel*. *Science* **238**, 692–694. (doi:10.1126/science.3118464)
51. Wolenski FS, Bradham CA, Finnerty JR, Gilmore TD. 2013 NF-κB is required for cnidocyte development in the sea anemone *Nematostella vectensis*. *Dev. Biol.* **373**, 205–215. (doi:10.1016/j.ydbio.2012.10.004)
52. Wang Y, Branicky R, Noë A, Hekimi S. 2018 Superoxide dismutases: dual roles in controlling ROS damage and regulating ROS signaling. *J. Cell Biol.* **217**, 1915–1928. (doi:10.1083/jcb.201708007)
53. Nii CM, Muscatine L. 1997 Oxidative stress in the symbiotic sea anemone *Aiptasia pulchella* (Carlgren, 1943): contribution of the animal to superoxide ion production at elevated temperature. *Biol. Bull.* **192**, 444–456. (doi:10.2307/1542753)
54. Gardner SG, Nielsen DA, Laczka O, Shimmon R, Beltran VH, Ralph PJ, Petrou K. 2016 Dimethylsulfoniopropionate, superoxide dismutase and glutathione as stress response indicators in three corals under short-term hyposalinity stress. *Proc. R. Soc. B* **283**, 20152418. (doi:10.1098/rspb.2015.2418)
55. Shore-Maggio A, Callahan SM, Aeby GS. 2018 Trade-offs in disease and bleaching susceptibility among two color morphs of the Hawaiian reef coral, *Montipora capitata*. *Coral Reefs* **37**, 507–517. (doi:10.1007/s00338-018-1675-0)
56. Muller EM, Bartels E, Baums IB. 2018 Bleaching causes loss of disease resistance within the threatened coral species *Acropora cervicornis*. *eLife* **7**, e35066. (doi:10.7554/eLife.35066)
57. Pinzón JH, Kamel B, Burge CA, Harvell CD, Medina M, Weil E, Mydlarz LD. 2015 Whole transcriptome analysis reveals changes in expression of immune-related genes during and after bleaching in a reef-building coral. *R. Soc. Open Sci.* **2**, 140214. (doi:10.1098/rsos.140214)
58. Augustin R, Fraune S, Bosch TCG. 2010 How *Hydra* senses and destroys microbes. *Semin.Immunol.* **22**, 54–58. (doi:10.1016/j.smim.2009.11.002)
59. Rosset S, Wiedenmann J, Reed AJ, D'Angelo C. 2017 Phosphate deficiency promotes coral bleaching and is reflected by the ultrastructure of symbiotic dinoflagellates. *Mar. Pollut. Bull.* **118**, 180–187. (doi:10.1016/j.marpolbul.2017.02.044)
60. Hughes TP *et al.* 2018 Spatial and temporal patterns of mass bleaching of corals in the Anthropocene. *Science* **359**, 80–83. (doi:10.1126/science.aan8048)
61. Valadez-Ingersoll M, Aguirre Carrión PJ, Bodnar CA, Desai NA, Gilmore TD, Davies SW. 2024 Starvation differentially affects gene expression, immunity and pathogen susceptibility across symbiotic states in a model cnidarian. Figshare. (doi:10.6084/m9.figshare.c.7075463)